Journal of Molecular Catalysis A: Chemical 348 (2011) 30–41

Contents lists available at ScienceDirect

Journal of Molecular Catalysis A: Chemical

journal homepage: www.elsevier.com/locate/molcata

Enantioselective hydrogenation of 1-phenyl-propane-1,2-dione on immobilised cinchonidine Pt/SiO_2 catalysts

Cristian H. Campos[a,*], Marcelo Oportus[a], Cecilia Torres[a], Claudia Urbina[a], José L.G. Fierro[b], Patricio Reyes[a,*]

[a] Edmundo Larenas 129/Universidad de Concepción, Departamento de Fisicoquímica, Laboratorio de Catálisis por Metales, Concepción, Chile
[b] Grupo de Energía y Quimica Sostenible, Instituto de Catálisis y Petroleoquímica, CSIC, C/Marie 2, Cantoblanco, 28049 Madrid, Spain

ARTICLE INFO

Article history:
Received 23 May 2011
Received in revised form 24 July 2011
Accepted 26 July 2011
Available online 10 August 2011

Keywords:
Heterogenisation
Platinum
Cinchonidine
1-Phenyl-propane-1,2-dione
Heterogeneous catalyst

ABSTRACT

Chirally modified SiO_2 containing different amounts of cinchonidine was prepared by the chemical modification of cinchonidine (CD) with trimethoxysilane over SiO_2 that had been chemically activated with 1,4-dioxane/HCl. This solid was used to support Pt catalysts containing 1 wt%Pt obtained by the chemical reduction of hexachloroplatinic acid with H_2 at 298 K and 40 bar. The materials were characterised by elemental analyses of C, H, and N, as well as thermal gravimetry (TG), DRIFT, ^{13}C NMR, ^{29}Si solid state NMR, N_2 adsorption–desorption at 77 K, X-ray diffraction (XDR), XPS, and HR-TEM. Catalytic activity for the hydrogenation of 1-phenyl-propane-1,2-dione was evaluated in a batch reactor at 298 K and 40 bar, and recycling of the catalysts yielding the largest enantiomeric excess in the products were also studied. All catalysts were found to be active in the reaction, with enantiomeric excesses of the target product (1-R-phenyl-1-hydroxy-2-propanone) ranging from 35 to 50%. The best catalyst studied was SiO_2-supported, with a nominal content of 7.5 mmolCD/L g. The recycling tests showed a loss of activity that was attributed to the surface modification of the catalyst.

1. Introduction

Catalytic enantioselective hydrogenation is one way to obtain enantiopure compounds from reducible moieties such as C=C, C=N, and C=O. For heterogeneous catalysis, supported noble metals that operate in the presence of a chiral auxiliary molecule are often used. The chiral auxiliary is generally a derivative of quinine, an alkaloid that presents three characteristic groups in its structure: a quinoline ring; an asymmetrical, bridge-type centre that incorporates a hydroxyl group; and a quinuclidine ring that can have a vinyl group (–CH=CH_2) on one of its vertices [1]. This inducer is generally added to the reaction system *in situ* and has been widely studied in hydrogenation reactions of α-keto esters and α-diketones [2–5]. Diverse metals such as Pt, Ir, Pd, Rh, and Ru supported on SiO_2, Al_2O_3, and others, have been used as an active phase. Cinchonidine (CD) has been the main chiral auxiliary used in hydrogenation studies of liquid phase ethyl pyruvate and 1-phenyl-propane-1,2-dione (PPD) [3,5–8].

A diverse range of improvements have been reported in the preparation of heterogeneous catalysts, including modifications of inorganic supports through the immobilisation of organometallic catalysts on SiO_2 and its derivatives [9]. Jamis et al. [10] described the encapsulation *via* sol–gel of organometallic complexes of Ru to be used in aqueous phase hydrogenations. Fan et al. proposed the use of insoluble polymers as supports for homogeneous catalysts immobilised by entrapment [11]. Complexes can also be supported through anchoring mediated by a coupling agent, typically trimethoxysilane derivatives functionalised with Cl, NH_2, or SH on materials such as Al_2O_3, La_2O_3, MCM-41, ZrO_2, TiO_2, or Fe_2O_3, among others [12–16].

The CD molecule, like organometallic complexes, can be anchored on the surface of a solid. Several authors have reported the anchoring of quinine derivatives on SiO_2 and other supports used as stationary phases in HPLC. Lämmerhofer et al. reported anchoring mediated by carbamates with the OH group at the C9 position [17], whereas Ma et al. used sulphur bridge-type bonds to immobilise quinines through the vinyl group of the quinuclidine ring [18]. Pesek et al. [21,22] studied the surface modification of SiO_2 with organic molecules, finding alkoxysilanes to be more versatile "coupling agents" (CA) for immobilising this type of substrate. The alkoxysilane was anchored by transesterification of the alkoxide groups, making the prior activation of the SiO_2 surface necessary due to the low quantity of OH groups found on the oxides typically used for catalysis and the ensuing low surface reactivity in this type of reaction [23–28]. The immobilisation of CD by means of

* Corresponding authors.
E-mail addresses: ccampos@udec.cl (C.H. Campos), preyes@udec.cl (P. Reyes).

1381-1169/$ – see front matter © 2011 Elsevier B.V. All rights reserved.
doi:10.1016/j.molcata.2011.07.016

the reaction between the CA and the anchored inducer have been reported [29,30] and in these studies it has been demonstrated that the presence of remaining groups of the CA on the support surface interfere in the catalytic performance [30]. If the chiral inducer is modified prior its immobilisation on the support surface it would allow a better control on the surface organic species, and therefore it is likely to assess that the anchored species correspond only to chiral inducer.

Modifications of CD were studied by the group of Toukoniitty [19,20], who introduced triethoxysilane groups into the vinyl group of the quinuclidine heterocycle and made multiple modifications to the hydroxyl group at C9 using various derivatives of chlorosilanes in enantioselective hydrogenation studies of PPD. According to those authors, modifications in the hydroxyl group heavily alter the capacity for enantioselectivity on the part of the chiral auxiliary. Thus, the inducer of chirality can be anchored on a supported metallic catalyst rather than adsorbed onto the active phase, potentially giving rise to systems reusable for consecutive batch cycles.

The presence of organic content on the surface of a support changes its thermal stability [31]. Therefore, catalysts with an immobilised organic molecule on the support must be prepared for surface metal deposition using an alternative to the traditional synthesis of supported metal catalysts (precursor impregnation, calcination, and reduction between 200 and 500 °C). Platinum has given the best results for both activity and selectivity in the hydrogenation of prochiral substrates and has been widely studied by Toukoniitty et al. [6,7,19,20,32,33]. Different physical and chemical methods have been used to prepare nanoscale Pt [34], including chemical reduction and stabilisation with polymers and oligomers [35] and electrostatic stabilisation [36], among others. For the synthesis of Pt colloids, Bönnemann and Braun [37] used formic acid as a reducing agent at 100 °C in the presence of CD as a stabilising agent. Roucoux et al. [38] assayed the activity of colloidal phases stabilised with surfactants under high pressure H_2 in the hydrogenation of α-keto esters. This methodology was used by Reyes et al. to support colloids on SiO_2, generating catalysts employed in the hydrogenation of ethyl pyruvate and PPD [39,40]. These authors found somewhat lower enantioselectivity in stabilised systems than that obtained when using an inducer adsorbed on the catalyst surface.

Our review of the literature has led us to propose the synthesis of catalysts *via* immobilisation of CD on the SiO_2 surface and dispersal of Pt over this modified support as an active phase obtained by the reduction of an inorganic precursor under high pressure H_2 during the hydrogenation of PPD under predetermined conditions.

2. Experimental

2.1. General

All air-sensitive reactions were performed in a Schlenk flask using an inert argon (Ar) atmosphere. Tetrahydrofuran (THF, Merck) was dried over metallic sodium/benzophenone; toluene (99%, Merck) was dried over metallic sodium; and triethylamine (TEA) was distilled at reduced pressure prior to use. CD (96%, Aldrich), trimethylchlorosilane (TMCS 98%, Merck), trimethoxysilane (TMS 98%, Merck), platinum cyclooctadienyl (II) chloride ($PtCODCl_2$, Aldrich), anhydrous sodium sulphate (Na_2SO_4, Merck), SiO_2 (Grace Davison), $H_2PtCl_6{\cdot}6H_2O$ (40%Pt, Merck), NaOH (Merck), and other solvents (Merck) were used as received.

Elemental analyses of C, H, and N were performed on a LECO CHNS-932 analyser. TG studies were performed with a Mettler Toledo Thermogravimetric TGA/SDTA 851 using an O_2 flow of 25 mL/min and a temperature ramp of 1 K/min from 298 to 1000 K. NMR spectra for ^1H and $^{13}C\{^1H\}$ were obtained on a Bruker AMX-300 spectrometer (300 MHz for ^1H, 75 MHz for ^{13}C) using trimethylsilane as a standard; all the results obtained from the NMR of ^1H and ^{13}C were compared with the results from Toukoniitty et al. [19,20] with respect to the observed allocations and dislodged chemical signals. Solid-state ^{13}C and ^{29}Si CP NMR spectra were recorded at 100.6 MHz and 79.49 MHz, respectively, using a Bruker AV 400 WB spectrometer. Diffuse reflectance infrared Fourier transform (DRIFT) spectra were obtained using a JASCO FT/IR-6300 spectrometer. XRD patterns were recorded on a RigakuD/max-2500 diffractometer with Cu K_α radiation at 40 kV and 100 mA. N_2 adsorption-desorption analysis was performed at 77 K on a Micromeritics ASAP 2010 apparatus. Specific surface areas were determined *via* the BET (Brunauer–Emmett–Teller) equation, using adsorption data in the relative pressure range of 0.05–0.3, and pore-size distributions were estimated using the BJH model. HR-TEM micrographs were obtained with a HR-TEM Philips CM-200 system. Photoelectron spectra (XPS) were recorded using an Escalab 200 R spectrometer equipped with a hemispherical analyser and using non-monochromatic Mg Kα X-ray radiation ($h\upsilon$ = 1253.6 eV). The surface Pt/Si and N/Si atomic ratios were estimated from the integrated intensities of Pt 4f, Si 2p, C 1s, and N 1s lines after background subtraction and correction by the atomic sensitivity factors [41]. The spectra were fitted to a combination of Gaussian–Lorentzian lines of variable proportions. The binding energy of the Si 2p peak at 103.4 eV was taken as an internal standard.

2.2. Activation of SiO_2

The surface activation of SiO_2 was performed in a round-bottom flask in which 3 g of SiO_2 was mixed with 24 mL of 1,4-dioxane and 3 mL HCl (3.1 mol/L). The mixture was stirred for 30 min at 353 K, filtered, and dried under vacuum for 4 h at 393 K.

2.3. Preparation of modified CD

The modification of CD and its subsequent hydrosilation were performed according to methods reported by Toukoniitty and co-workers [19]. An ice-cooled solution of CD (2.5 g, 8.5 mmol) in THF containing TEA (1.2 mL, 8.5 mmol) was added dropwise to TMCS (1.0 mL, 8.5 mmol). The reaction mixture was stirred for 20 h at room temperature and then for 2 h at 60 °C. The product was extracted with chloroform (50 mL) and washed with water (3× 50 mL). The water layer was extracted with additional chloroform (50 mL) and the combined organic extracts were dried over sodium sulphate. Evaporation of the solvents left 2.5 g of solid (label CD-9-O) (see Scheme 1). ^1H NMR ($CDCl_3$, δ): 8.93 (d, 1H, H-2′), 8.19 (dd, 1H, H-8′), 7.81 (br, 2H, H-5′, H-7′), 7.55 (ddd, 1H, H-6′), 7.30 (br, 1H, H-3′), 5.62 (ur, 2H, H-9, H-10), 5.07 (ur, 2H, H-11), 3.31 (ur, 1H, H-6b), 3.15 (ur, 2H, H-2a, H-8), 2.68 (ur, 1H, H-7b), 2.43 (m, 1H, H-6a), 2.11 (ur, 2H, H-2b, H-3) 1.89 (m, 1H, H-4), 1.49 (m, 1H, H-5b), 1.29 (m, 1H, H-5a), 0.85 (m, 1H, H-7a), 0.18 (s, 9H, Si–CH_3). ^{13}C NMR ($CDCl_3$, δ): 149.59 (C-2′), 148.38 (C-8a′), 146.20 (C-4′), 138.00 (C-10), 130.23 (C-8′), 129.72 (C-7′), 128.10 (C-6′), 124.72 (C-4a′), 123.52 (br, C-5′), 118.61 (br, C-3′), 116.84 (C-11), 68.74 (br, C-9), 60.84 (C-8), 56.70 (C-2), 43.06 (br, C-6), 35.49 (C-3), 29,69 (C-4), 27.12 (C-5), 18.62 (br, C-7), 0.35 (3C, Si–CH_3).

2.4. Hydrosilation of modified CD

$PtCODCl_2$ (0.018 g, 0.049 mmol) and TMS (0.77 mL, 6.0 mmol) were added at 313 K to a solution of CD-9-O (2.0 g prepared according to the previous reaction, approx. 5.5 mmol) in toluene (20 mL). The reaction mixture was stirred for 5 h at 363 K under a N_2 atmosphere. Purification by flash chromatography (hexane–acetone–TEA, 40:18:1) gave 1.25 g of the desired product as a yellowish amorphous material (TMS-CD-9-O). ^1H NMR ($CDCl_3$,

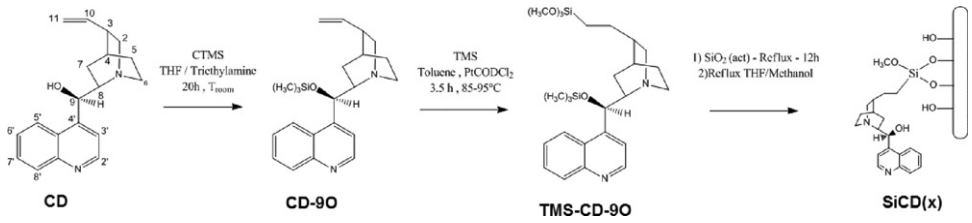

Scheme 1. Synthetic route for CD modification.

δ): 8.88 (d, 1H, H-2′), 8.14 (dd, H-8′), 7.76 (br, 2H, H-5′, H-7′), 7.50 (ddd, 1H, H-6′), 7.26 (br, 1H, H-3′), 5.61 (br, 1H, H-9), 3.95 (q, 6H, J = 7.0 Hz, $SiOCH_3$), 3.39 (ur, 1H, H-6b), 3.03 (ur, 2H, 1H, H-8), 2.66 (ddd, H-6a), 2.21 (ur, 1H, H-2b), 2.03–1.78 (ur, 3H, H-4, H-5b, H-7b), 1.41 (ur, 1H, H-3), 1.24 (m, 1H, H-10), 1.24–1.16 (ur, 2H, H-5a, H-7a), 1.22 (m, 2H, H-11), 0.80 (s, 9H, Si–CH_3). ^{13}C NMR ($CDCl_3$, δ): 149.63 (C-2′), 148.40 (C-4′ or C-8a′), 146.05 (C-4′ or C-8a′), 130.28 (C-8′), 129.77 (C-7′), 128.23 (C-6′), 124.69 (C-4a′), 123.77 (br, C-5′), 118.59 (br, C-3′), 68.60 (br, C-9), 60.98 (C-8), 60.69 (C-2), 56.85 (3C, $SiOCH_3$), 43.03 (br, C-6), 35.67 (C-3), 27.32 (C-5), 27.02 (C-10), 25.29 (C-4), 24.77 (br, C-7), 11.49 (C-11), 0.34 (3C, Si–CH_3).

2.5. Synthesis of modified SiO_2

Five supports were prepared with different amounts of CD (0.5, 2.5, 5.0, 7.5, or 10 mmol/L $g_{support}$), simulating the CD fractions that are added in traditional systems (range: 0.5–10 mmol/L $g_{support}$). Two grams of activated SiO_2 and the necessary quantity of TMS-CD-9-O dissolved in toluene were placed in a round-bottom flask, and the volume of the system was raised to 50 mL with toluene. The reaction was refluxed for 12 h and subsequently filtered and washed two times with 40 mL toluene and 20 mL chloroform. The solid was dried in a furnace for 1 h at 353 K. The solid obtained was treated by refluxing it in a mixture of methanol/THF for 20 h and was then washed with 100 mL of n-pentane. Finally, the solids were dried under vacuum for 4 h at 120 °C. All the samples of modified supports were tabulated as SiCD(x), where x is the nominal concentration (10^{-3} mmol CD/g L).

2.6. Catalyst preparation

The catalyst (1 g) was prepared at 1%Pt mass using the five modified supports and activated SiO_2. These are denoted 1%Pt/TMS-CD(x), where x: 0–10. The methodology is analogous to that reported by Roucoux et al. [38]. The support plus the necessary quantity of $H_2PtCl_6{\cdot}6H_2O$ and a stoichiometric quantity of NaOH (0.5 mol/L) were added to a batch reactor equipped with a Teflon cup. The pressure was adjusted to 40 bar H_2 and the mixture was reacted for 2 h with constant magnetic stirring to obtain the reduced supported metal. The solid was filtered and washed to a constant pH and conductivity. Finally, it was dried in a furnace at 373 K for 1 h.

2.7. Catalytic activity

The catalytic assays for PPD hydrogenation were performed in a stainless steel Parr-type batch reactor at a concentration of 0.01 mol/L of substrate using cyclohexane as a solvent and stirring at 600 rpm under 40 bar H_2 pressure. Analyses of reactants and products were followed by gas chromatography mass spectrometry using a GC–MS instrument (Shimadzu GCMS-QP5050) with chiral β-Dex 225, a 30-m column (Supelco), and helium as the carrier gas. The recycling assays were performed by filtering the catalyst from the reaction medium. The filtered catalyst was washed three times consecutively with chloroform to clean the surface and then dried at 373 K for 24 h before reuse.

3. Results and discussion

3.1. Synthesis and characterisation of the precursor and supports

The synthetic route for CD modification utilises a silane ether at the hydroxyl group of carbon 9 in order to protect the stereogenic centre responsible for enantioselectivity, as reported by other authors [1,19,32]. The $PtCODCl_2$ catalyst is known to be a good alternative to Karstedt's catalyst and to H_2PtCl_6, the two most studied catalysts, and the use of TMS-CD-9-O resulted in hydrosilation yields of around 60% due to the addition of TMS. Several authors [31,42,43] have shown that activation of the vinyl group can be achieved using both of the carbons of the C=C bond, forming an α-adduct when the addition is by a methylene carbon or a β-adduct if by addition of a methylene carbon. In the present study, the catalyst was 100% selective in the addition of CD at C11 (α-adduct).

SiO_2 activation was performed primarily to enrich the surface in the Si–OH groups that are responsible for anchoring TMS-CD-9-O, as reported by Pesek et al. [21,22]. Once anchored on the surface of the solid, the C9 hydroxyl group was deprotected. This was achieved by refluxing the solid with methanol for 24 h, displacing the trimethylsilane group to recover the OH group. Table 1 summarises the elemental analyses of the supports. The total content of CD anchored on the surface was lower than the nominal content, and the decrease in anchoring became more pronounced as the nominal content of the modifier increased. This could be explained by diffusion phenomena in the anchoring reactions, as increasing the degree of coverage by TMS-CD may hinder access to the methoxy groups of the coupling agent at the SiO_2 surface due to the steric impediment of the quinuclidine and quinoline rings belonging to the previously anchored molecules and to other steric conflicts generated during the deprotection treatment. As indicated by Blümel and other authors [44–46], species of the type $(CH_3)_3$–$SiOCH_3$ were formed that were able to exchange with the surface silanol groups as well as the methanol. Thus, we based our calculations on N (%), the only true indicator of TMS-CD content anchored on SiO_2. The anchoring of impurities by the deprotection treatment, in addition to the contribution by the exchange phenomenon, was one of the reasons for the high C (%) and H (%) values found in the samples relative to the nominal C/N (see Fig. 1). Fig. 1 shows the distribution of the atomic ratios determined by elemental analysis (at.%). At low TMS-CD contents, organic matter was enriched and as the surface content increased, the C/N ratio declined, falling below stoichiometric values and reaching nominal values above 5.0 mmol CD/L g. The H/N ratio was always greater than the calculated value due to the surface activation.

To explain the apparent loss of C (%), we studied the TG of the precursor and the supports in an oxidising atmosphere, simulating the process of elemental analysis. Fig. 2 shows the curves of weight loss in percentage of mass as a function of the temperature for TMS-CD and the various synthesized supports. It should be noted that the species anchored on the support was TMS-CD-9-O,

Table 1
Elemental analysis of supports, catalysts, and cycles studied in the enantioselective hydrogenation of PPD.

Sample	C (%)	H (%)	N (%)	Concentration (10^{-4} mol/L g)	Yield (%)
SiCD(0.5)	1.73	0.52	0.06	0.43	85.7
	1.02[a]	0.40[a]	0.06[a]	0.42[a]	82.1[a]
SiCD(2.5)	3.87	0.70	0.29	2.0	81.4
	2.12[a]	0.62[a]	0.26[a]	1.8[a]	72.9[a]
SiCD(5.0)	5.00	0.94	0.53	3.8	75.0
	3.05[a]	0.70[a]	0.38[a]	2.7[a]	54.3[a]
SiCD(7.5)	5.50	1.06	0.69	5.0	65.2
	4.01[a]	0.82[a]	0.51[a]	3.6[a]	48.1[a]
	3.97[b,1]	0.85[b,1]	0.45[b,1]	3.2[b,1]	89.1[b,1]
	4.83[b,2]	0.94[b,2]	0.42[b,2]	3.0[b,2]	82.2[b,2]
	5.63[b,3]	1.01[b,3]	0.41[b,3]	2.9[b,3]	80.2[b,3]
	7.04[b,4]	1.17[b,4]	0.41[b,4]	2.9[b,4]	80.2[b,4]
	9.06[b,5]	1.30[b,5]	0.40[b,5]	2.8[b,5]	79.2[b,5]
SiCD(10)	5.76	1.10	0.72	5.1	51.4
	4.29[a]	0.85[a]	0.55[a]	3.9[a]	38.9[a]

[a] Catalysts at 1 wt%Pt.
[b] [x]Reused catalysts, where *x* corresponds to the run number and 5 is the catalyst recovered from the last cycle.

and the TG of the TMS-CD species obtained with the TMS-CD-9-O treatment was performed under the same conditions as that of the synthesized supports. The curve obtained for the TMS-CD precursor showed thermal stability to approximately 473 K, at which point the precursor began to lose mass, passing through an intermediate stage (620–670 K) in which it was assumed to have lost most of the aliphatic fraction. The aromatic fraction began to react at higher temperatures, forming intermediate species of the type SiC_xO_y, leaving approximately 18% at 770 K that was highly stable at temperatures greater than 1270 K, as reported by Schiavon et al. [47]. In relation to the supports, we noted that SiO_2 had a low quantity of surface OH groups and once the support was activated, mass was lost due to an increase in the surface concentration of Si–OH. A drop in the curves of the heterogenised supports with TMS-CD was also found and attributed to the loss of organic matter from the TMS-CD functionalities, analogous to that found for the pure precursor, exhibiting initial decomposition temperatures to values close to 523 K in the case of SiCD(10).

Fig. 3 shows the DRIFT spectra of the synthesized supports. In the case of SiCD(0.0), we observed an intense band around 3500–4000 cm^{-1} corresponding to the stretching vibration mode of the hydroxyl groups of activated SiO_2. As the TMS-CD was anchored to the solid, the band decreased and vibrations corresponding to C–H bonds appeared at frequencies of 3000–2900 cm^{-1}. These bands increased in intensity along with the content of organic matter on the solid. A distinct band appeared between 1400 and 1500 cm^{-1} corresponding to vibrations of $Si–CH_3$ bonds. This band was attributed to the trimethylsilane species (impurities) anchored on the surface of the support, as verified by NMR of the solids (see Fig. 4). Fig. 4(a) shows an unusual band of chemical shifts between −1.0 and −2.0 ppm corresponding to $Si–CH_3$ species in

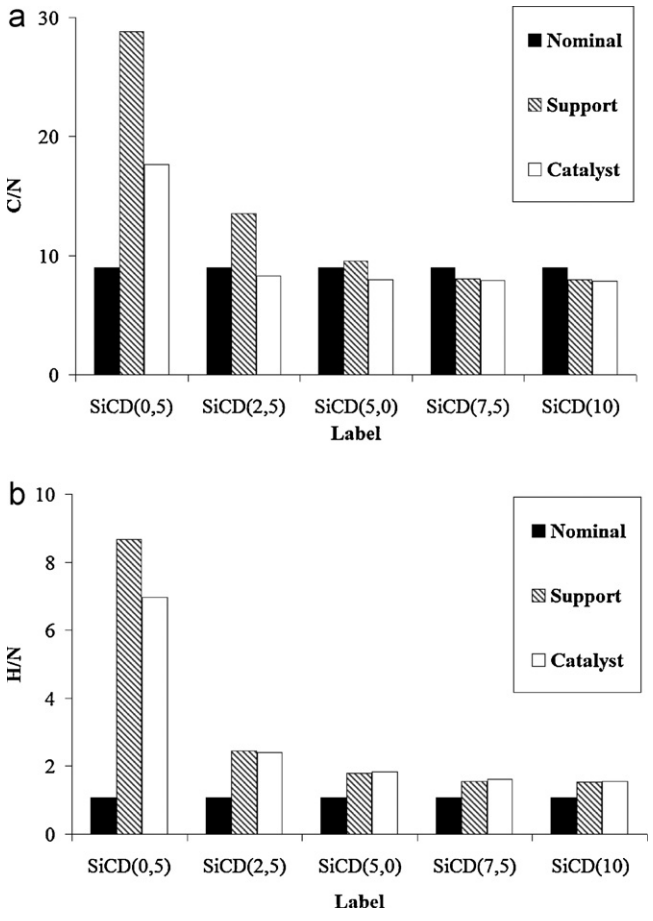

Fig. 1. Distribution of atomic ratios determined by percentage of atoms detected by elemental analysis on the supports and synthesized catalysts by anchoring of TMS-CD. (a) C/N and (b) H/C.

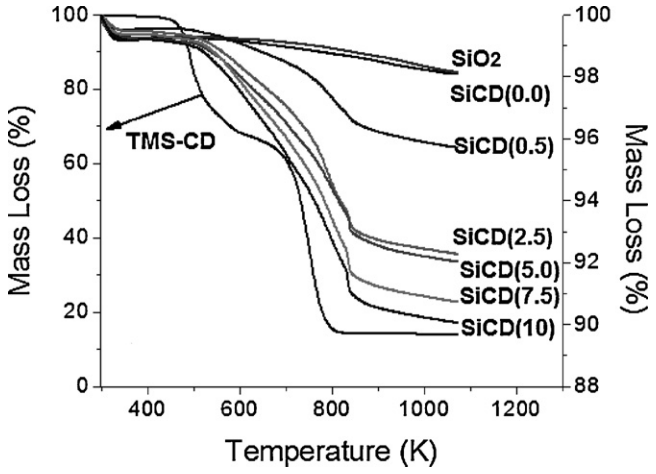

Fig. 2. TG curves for the synthesis supports. Conditions: O_2 atmosphere to 25 mL/min flow and temperatures 298–1000 K.

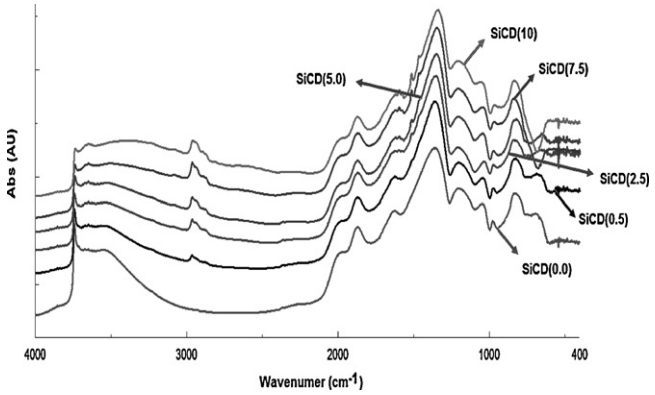

Fig. 3. DRIFT of the supports modified with TMS-CD.

all the samples and a significant increase of characteristic bands of the aromatic and aliphatic region corresponding to TMS-CD as the loading increased. Fig. 4(b) shows the characteristic signal of SiO_2 corresponding to an atom of Si tetracoordinated by atoms of O from the network (−100 ppm) and split due to the activation of the support. As the TMS-CD content increased on the surface, this splitting became less significant and, as reported by Yu et al. [46], the characteristic signals of anchoring of the types T^2 and T^3 at shifts between −50 and −80 ppm began to appear. A signal between 13 and 14 ppm, typical of CH_3–Si–O–Si species, was found for all the supports. This finding, when taken together with the DRIFT and ^{13}C NMR data, is indicative of the presence of impurities (trimethylsilane derivatives) that reacted with surface silanols in the deprotection treatment.

Analysis of N_2 adsorption–desorption isotherms and S_{BET} showed that all the solids were mesoporous and had type IV hysteresis cycles, corresponding to cylindrical pores (Fig. 5). Moreover, all samples presented monomodal pore-size distributions. Table 2 shows the surface areas and average pore diameters of the prepared solids. This information allows us to infer that as the TMS-CD content increased on the supports, the values for surface area, pore volume, and pore size decreased due to the anchoring of the organic molecule on the surface of the activated SiO_2.

3.2. Catalyst synthesis and characterisation

The catalysts were synthesized by H_2 reduction of a soluble platinum precursor using a pressure of 40 bar as reported by Roucoux et al. [38]. The reaction at room temperature allowed us to obtain

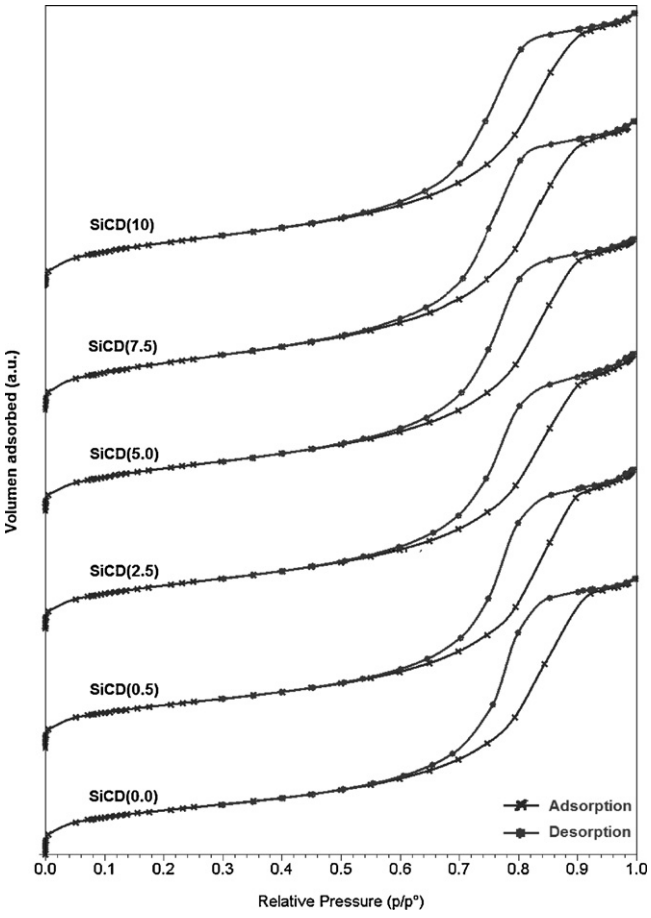

Fig. 5. N_2 adsorption–desorption isotherms of 77 K on Pt/SiCD(x) catalysts.

the chiral auxiliary in open conformation 3, which is the optimum for enantioselectivity, as reported by Baiker et al. [2]. The stoichiometric addition of NaOH to the system allowed us to obtain a neutral medium at the end of the reduction. H_2 oxidises to H^+, leaving an acid medium that could interact with the basic N of the quinuclidine ring of the anchored inducer if not neutralised. Table 1 summarises the values obtained for the surface concentration of the modifier on the catalysts. We noted a drop in the TMS-CD content in relation to the pure support attributable to the catalyst preparation conditions, which involved leaching of the inducer and the corre-

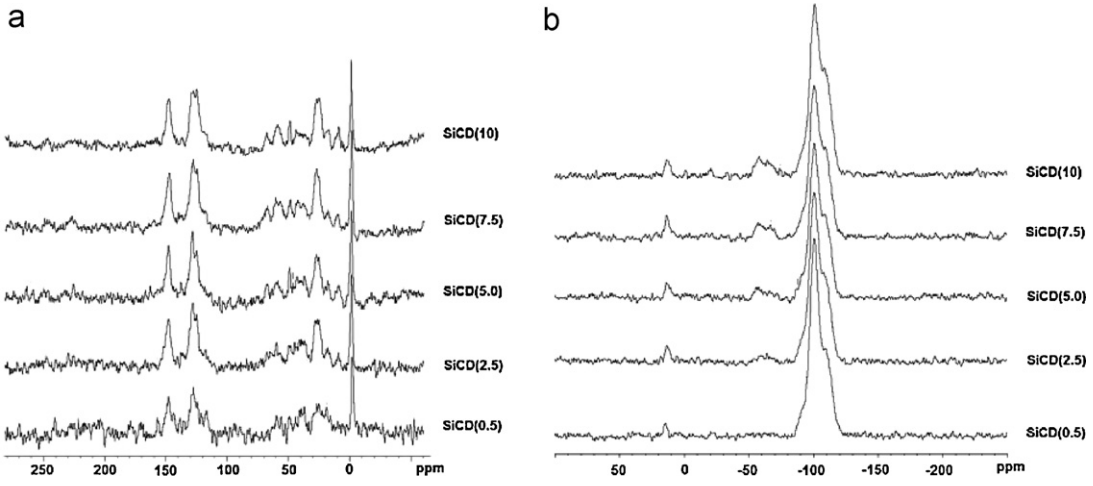

Fig. 4. NMR of the supports modified with TMS-CD. (a) ^{13}C and (b) ^{29}Si (CP).

Table 2
Surface area, pore volume, average pore diameter and metal particle size of 1 wt%Pt/SiCD(x) catalysts.

Catalyst	S_{BET} ($m^2\ g^{-1}$)	Pore volume ($cm^3\ g^{-1}$)	Average pore diameter (nm)	d_{XRD} [a] (nm)	$d_{p\ TEM}$ [a] (nm)
Pt/SiCD(0.0)	337	0.88	10.6	10.0	9.6
Pt/SiCD(0.5)	306	0.82	10.4	7.5	8.0
Pt/SiCD(2.5)	300	0.75	10.2	6.8	4.3
Pt/SiCD(5.0)	296	0.75	10.1	6.0	3.4
Pt/SiCD(7.5)	288	0.71	9.8	5.7	3.0
Pt/SiCD(10)	282	0.69	9.7	5.3	2.6

[a] Catalyst data.

sponding impurities. The C (%) and H (%) contents decreased, as did those of N (%), since H_2 is capable of reducing the $(CH_3)_3$–Si–O–Si groups anchored to SiO_2, releasing impurities and recovering the silanol groups [48] and the basic medium is able to interact with the anchored Si–O–Si bonds, releasing TMS-CD to a lesser degree than observed for the impurities. Despite the clean surface of the support during the catalyst preparation, the C/N ratio decreased, coming quite near the nominal C/N values for SiCD(0.5) to SiCD(5.0). The anchoring of impurities on SiCD(7.5) and SiCD(10) were further from the nominal values, as shown in Fig. 1. In all cases, the H/N ratio was comparable because the catalyst suffered a loss of impurities along with organic H. However, in all the cases, the H:N content was always higher than the nominal values.

The DRIFT spectra and N_2 adsorption–desorption isotherms of the supports and catalysts did not exhibit significant differences, so the crystalline nature of the active phase dispersed in the support was studied by XRD (Fig. 6). Note the characteristic Pt diffraction lines in the region of $2\theta \sim 40^\circ$. As the TMS-CD content at the surface increased, the lines diminished in intensity, becoming less clear. This was attributed to a higher dispersion of the active phase on the surface of the support. The metal particle size, shown in Table 2, was determined by XDR and TEM. All the catalysts exhibited metallic particle sizes smaller than 10 nm. With HR-TEM, similar values were obtained, as can be seen in the micrograph in Fig. 7. When the catalyst was prepared on the activated support, particle sizes were larger, reaching approximately 9.6 nm and a wider distribution of particle sizes was observed. When TMS-CD was anchored to the support, the average sizes declined as the organic molecule provided stability to the Pt cluster formed during the metal reduction, supporting the formation of smaller-sized agglomerates. Given these catalyst preparation conditions, we expected the nanoparticles to show a preferential orientation towards the sites modified with TMS-CD.

Fig. 8 shows the XPS core-level spectra obtained for the catalysts. The peak corresponding to Pt^0 at a BE of 71.0 eV was visible in all the spectra. With greater TMS-CD contents, the peak of species of the type $Pt^{\delta+}$ became more intense, due mainly to the interaction of the particles protected by TMS-CD with the N atoms of the modifier [39,40]. A decrease was observed in the Pt/Si surface ratio due to the surface coverage of SiO_2 by TMS-CD at nominal contents higher than 5.0 mmol CD/Lg, as shown in Table 3. Nonetheless, the N/Si ratio increased with the CD content at the surface, as shown by AE and DRIFT. The decline of the atomic ratio of Pt/N in the catalysts suggests that as the TMS-CD content on the surface increased, nanoparticles were deposited on sites around the anchoring sites, causing a decrease in metallic particle size, as observed by XRD and TEM.

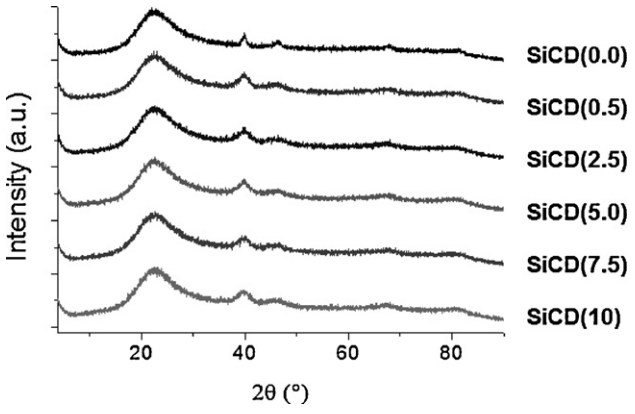

Fig. 6. XRD patterns of the catalysts synthesized on modified supports.

According the characterisation results strong interaction between the active phase and TMS-CD should be expected because of the significant changes in the metal particle size due to their preferential deposition on the modified sites of the chiral inducer.

3.3. Catalytic activity

Fig. 9 shows catalytic activity curves. For all catalysts, the activity varied with the TMS-CD content in the support. In all the cases, we found pseudo-first-order kinetics with respect to PPD, reaching conversion levels over 90% after 240 min for the catalysts 1%Pt/SiCD(x) with $x > 0.5$ and below 60% for those of $x < 0.5$. Scheme 2 shows the hydrogenation reaction of the carbonyl groups of the substrate. All the catalysts were selective for (R)-1-hydroxy-1-phenylpropan-2-one (1R-FP) and (S)-1-hydroxy-1-phenylpropan-2-one (1S-FP). Products of over hydrogenation were not detected.

The catalyst Pt/SiCD(0.0) showed the least activity, mostly due to the large size of the Pt crystals. A similar character was observed in the case of 1%Pt/SiCD(0.5): using DRIFT, ^{29}Si NMR, and S_{BET}, the surface characteristics of this catalyst were found to differ minimally from those of the activated support. However, it displays higher conversion due to the smaller-sized Pt crystals because, as discussed earlier, the anchoring of TMS-CD helped improve the dispersion of the active phase on the support. In parallel, this catalyst exhibits the deposition of impurity moieties which may be considered poisons. These can interfere with the adsorption of the substrate in the modified active phase (see Scheme 3), as reported in analogous studies of the anchoring of silane derivatives on Pt catalysts [49]. Although S_{BET} decreased as the quantity of anchored TMS-CD increased, there was a decline in the average metallic particle size. The resulting stabilisation effect allowed the deposition of smaller-sized nanoclusters, which increased the conversion levels (Table 4) and the rate constants, k_g. The increased rates with increased anchoring of TMS-CD on the supports can clearly be observed. The catalysts supported on SiCD(x) with $x > 0.5$ exhibited the highest conversion, reaching 97% in the case of SiCD(7.5). This was justified by the lower-than-nominal C/N ratios, denoting higher surface poisoning by impurities, in turn suggesting more expeditious surfaces for active site–substrate interactions during hydrogenation.

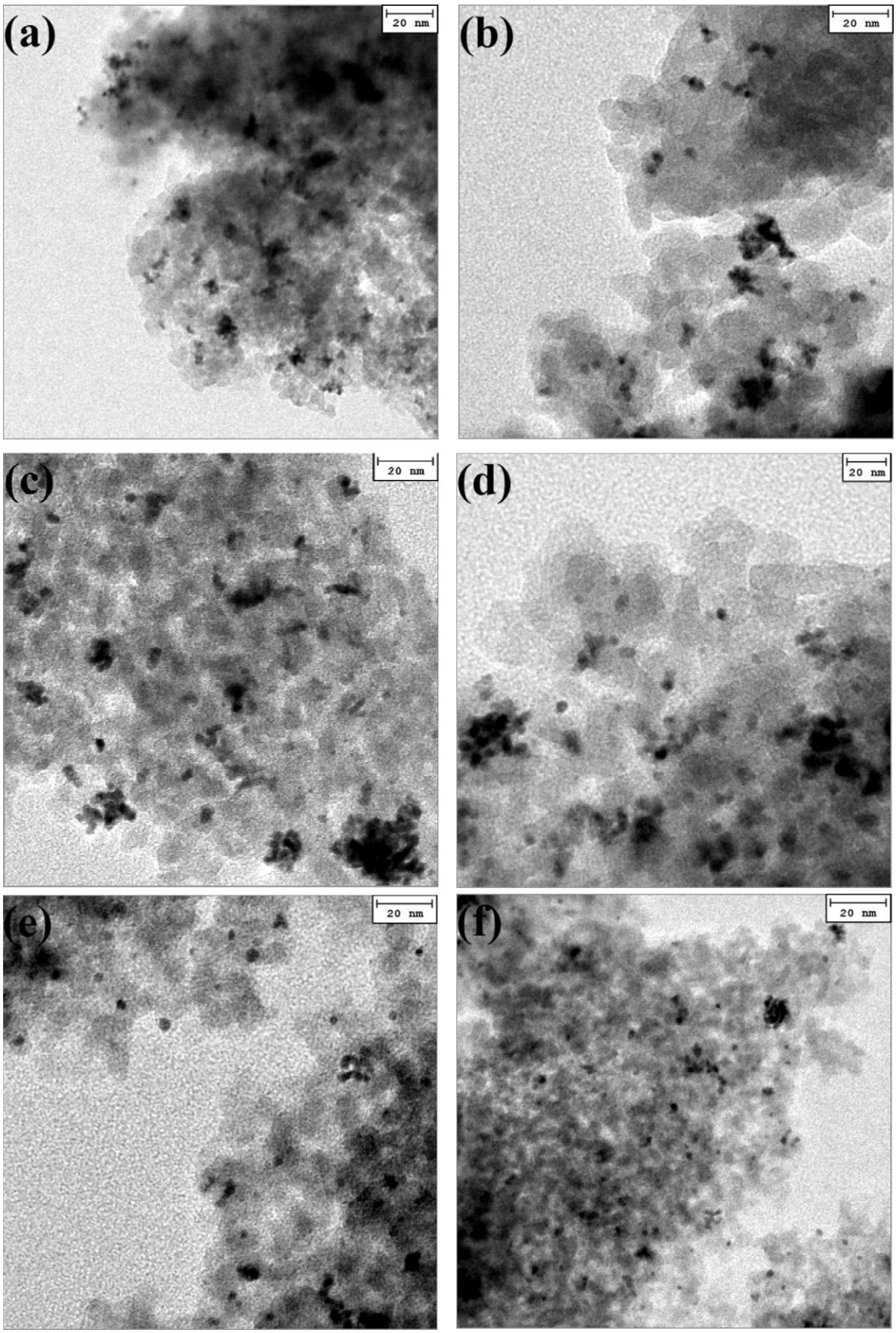

Fig. 7. TEM micrograph of the catalysts 1 wt%Pt supported on the modified SiO_2 (a) SiCD(0.0); (b) SiCD(0.5); (c) SiCD(2.5); (d) SiCD(5.0); (e) SiCD(7.5) and (f) SiCD(10).

Table 3
Binding energies (eV) of internal electrons and atomic surface ratio of 1wt%Pt/SiCD(*x*) catalysts.

Catalyst	Pt $4f_{7/2}$ (eV)	N 1s (eV)	Si 2p (eV)	Pt/Si at	N/Si at	Pt/N at
Pt/SiCD(0.0)	71.9 (94) 73.7 (6)	399.5 (64) 401.8 (36)	103.4	0.0025	–	–
Pt/SiCD(0.5)	71.9 (93) 73.9 (7)	399.4 (67) 401.7 (33)	103.4	0.0133	0.0194	0.685
Pt/SiCD(2.5)	71.9 (82) 73.9 (18)	399.4 (71) 401.9 (29)	103.4	0.0084	0.0312	0.269
Pt/SiCD(5.0)	72.0 (77) 73.8 (23)	399.5 (62) 401.8 (38)	103.4	0.0104	0.0409	0.254
Pt/SiCD(7.5)	72.0 (83) 73.8 (17)	399.5 (65) 401.9 (35)	103.4	0.0069	0.0490	0.168
Pt/SiCD(10)	71.9 (77) 73.6 (23)	399.5 (63) 401.9 (37)	103.4	0.0070	0.0503	0.139

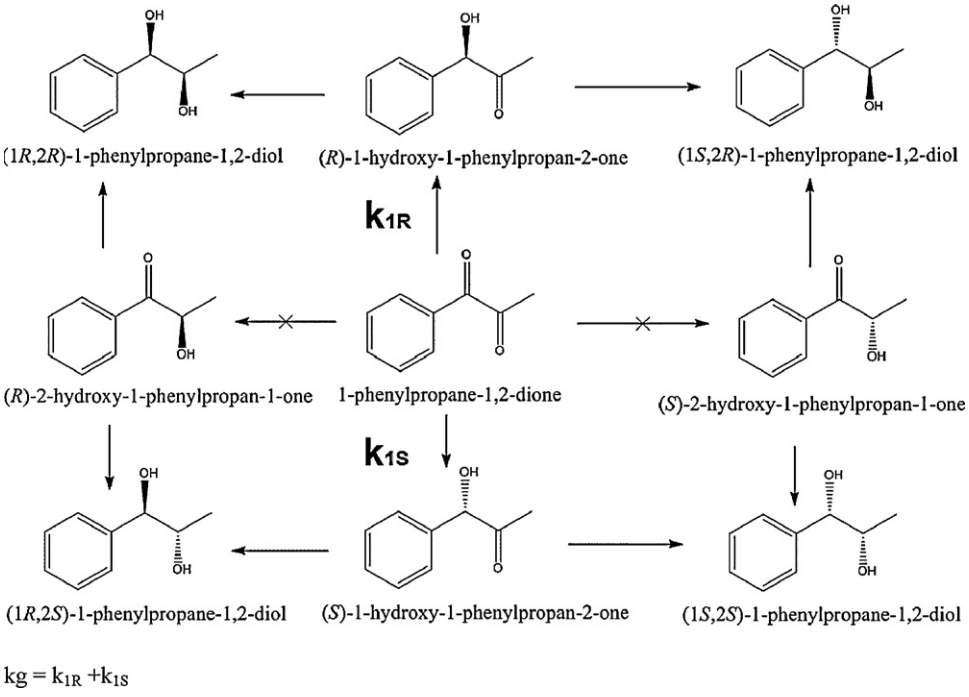

Scheme 2. Hydrogenation route of 1-phenylpropane-1,2-dione.

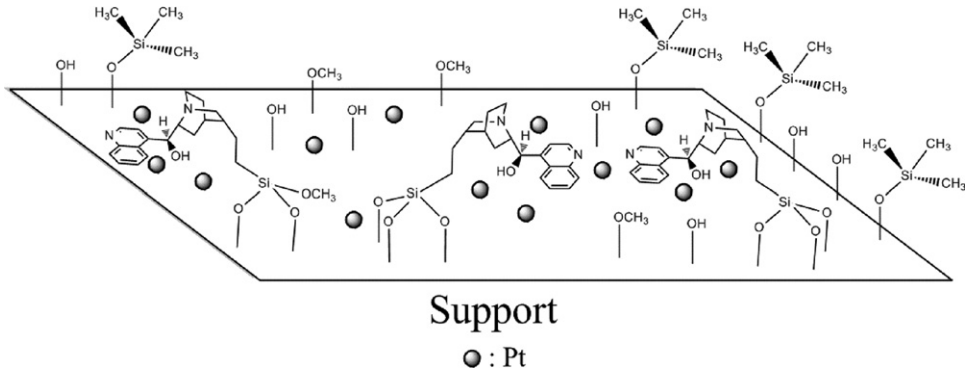

Scheme 3. Model of catalyst surface.

Table 4
Catalytic data for PPD hydrogenation. Reaction conditions: PPD concentration: 0.01 mol/L, P_{H_2} : 40 bar, stirring speed: 700 rpm.

Catalyst	k_g (10^2 min^{-1} g^{-1})	Conversion[a] (%)	ee max (%)
Pt/SiCD(0.0)	3.7	56	–
Pt/SiCD(0.5)	8.2	67	37
Pt/SiCD(2.5)	41.7	95	45
Pt/SiCD(5.0)	48.9	95	42
Pt/SiCD(7.5)	68.3	97	47
Pt/SiCD(10)	67.6	96	40

[a] At 4 h of reaction.

In relation to the selectivity of the catalysts, enantiomeric excess and regioselectivity have been defined as:

$$\text{ee}\,(\%) = \frac{[\text{R}] - [\text{S}]}{[\text{R}] + [\text{S}]} \cdot 100$$

$$\text{rs} = \frac{[\text{R}_{C1}] + [\text{S}_{C1}]}{[\text{R}_{C2}] + [\text{S}_{C2}]}$$

where [R] and [S] correspond to the concentrations of the respective enantiomers and in the case of rs, to the alcohols of the different carbonyl groups. Fig. 10 shows the curves of enantiomeric excess as a function of the conversion. All the catalysts were 100% selective for the hydrogenation of C=O adjacent to the phenyl group (see Scheme 2), giving 1R-FP as a product and an ee similar to the results reported for systems in which the chiral auxiliary was added *in situ* and adsorbed on the surface of the catalyst [50,51]. As the TMS-CD content on the surface increased, the ee also increased, reaching a maximum of 49% for the catalyst 1%Pt/SiCD(7.5), the most active and enantioselective. This was due mainly to the polarisation caused by the inducer on the Pt nanoparticle. Upon increased TMS-CD content, more $Pt^{\delta+}$ species were observed by XPS (see Fig. 8), favouring the selectivity of the product of interest.

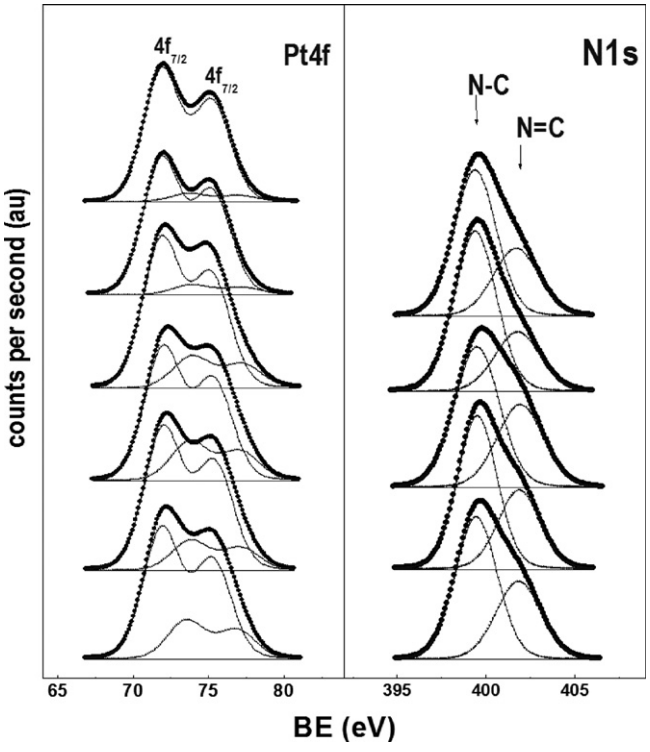

Fig. 8. XPS spectra for the catalysts supported on SiCD(*x*).

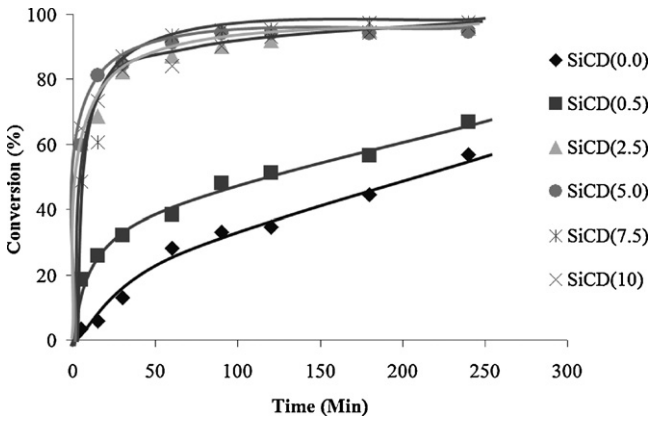

Fig. 9. Activity curves based on PPD for all the synthesized catalysts. Reaction conditions: PPD concentration: 0.01 mol/L, catalyst mass: 0.050 g, P_{H_2} : 40 bar, mixing speed: 700 rpm, solvent: cyclohexane.

3.3.1. Recycling studies

The catalyst supported on SiCD(7.5) exhibited the highest ee and was selected for assays of stability, activity, and selectivity in consecutive batch cycles. Between cycles, the catalyst was washed with chloroform in order to dissolve most of the organic matter that could be adsorbed on the support. The studied catalysts were characterised after each catalytic cycle by AE and XPS and the obtained results are compiled in Table 5. In the case of TMS-CD leaching, the organic matter was eliminated, as it is known to be highly soluble in this solvent [2]. C (%) and H (%) were found to increase after recycling. This was attributed to intermediate species of the support with 1R-FP and 1S-FP that appeared during the formation of bonds of the type Si–O–R, as reported by Blümel [44] and/or to the presence of species heavily adsorbed from the substrate, products, and/or solvent. N (%) decreases gradually along the catalytic cycles, which is assigned to a partial leaching of the inducer. XPS shows the presence of two types of surface nitrogen which may be assigned to aliphatic (399.5 eV) and aromatic nitrogen (401.8 eV) according Gammon et al. [52]. The inducer lost by leaching is not re-adsorbed on the metallic sites because no changes in the binding energy of the aromatic nitrogen was detected. On the other hand, the remaining anchored chiral inducer is slightly hydrogenated in the quinolline cycle of the TMS-CD as revealed the observed enhancement in the aliphatic/aromatic ratio, as shown in Scheme 4. The $Pt/Pt^{\delta+}$ atomic surface ratio remains constant along the cycles

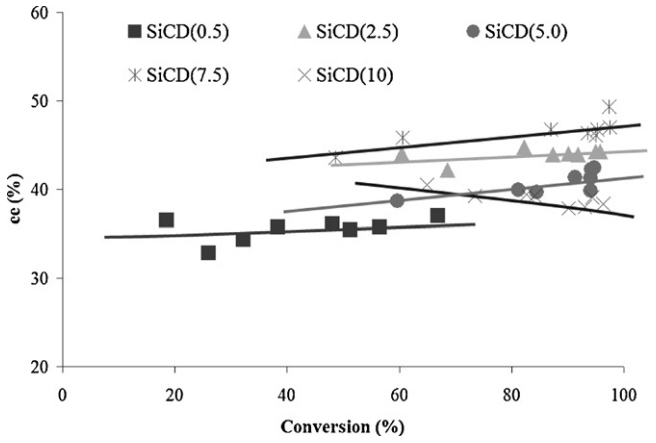

Fig. 10. Curves of enantiomeric excess in function of the conversion of PPD for all the synthesized catalysts. Reaction conditions: PPD concentration: 0.01 mol/L, catalyst mass: 0.050 g, P_{H_2} : 40 bar, mixing speed: 700 rpm, solvent: cyclohexane.

Table 5
Elemental analysis and XPS data of 1%Pt/SiCD(7.5) catalysts for cycles studies in the enantioselective hydrogenation of PPD.

Run	C (%)	H (%)	N (%)	Concentration (10^{-4} mol/L g)	N 1s (eV)	Pt $4f_{7/2}$ (eV)	N/Si at	Pt/Si at
0	4.01	0.82	0.51	3.6	399.5 (65) 401.9 (35)	72.0 (83) 73.8 (17)	0.049	0.0069
1	3.97	0.85	0.45	3.2	399.6 (64) 401.8 (36)	71.9 (79) 73.9 (21)	0.049	0.0069
2	4.83	0.94	0.42	3.0	399.6 (68) 401.8 (32)	71.9 (79) 73.9 (21)	0.048	0.0064
3	5.63	1.01	0.41	2.9	399.6 (70) 401.8 (30)	71.9 (75) 74.0 (25)	0.049	0.0065
4	7.04	1.17	0.41	2.9	399.5 (71) 401.8 (29)	72.0 (78) 74.0 (22)	0.038	0.0052
Final	9.06	1.30	0.40	2.8	399.5 (74) 401.8 (26)	71.9 (75) 73.9 (25)	0.037	0.0038

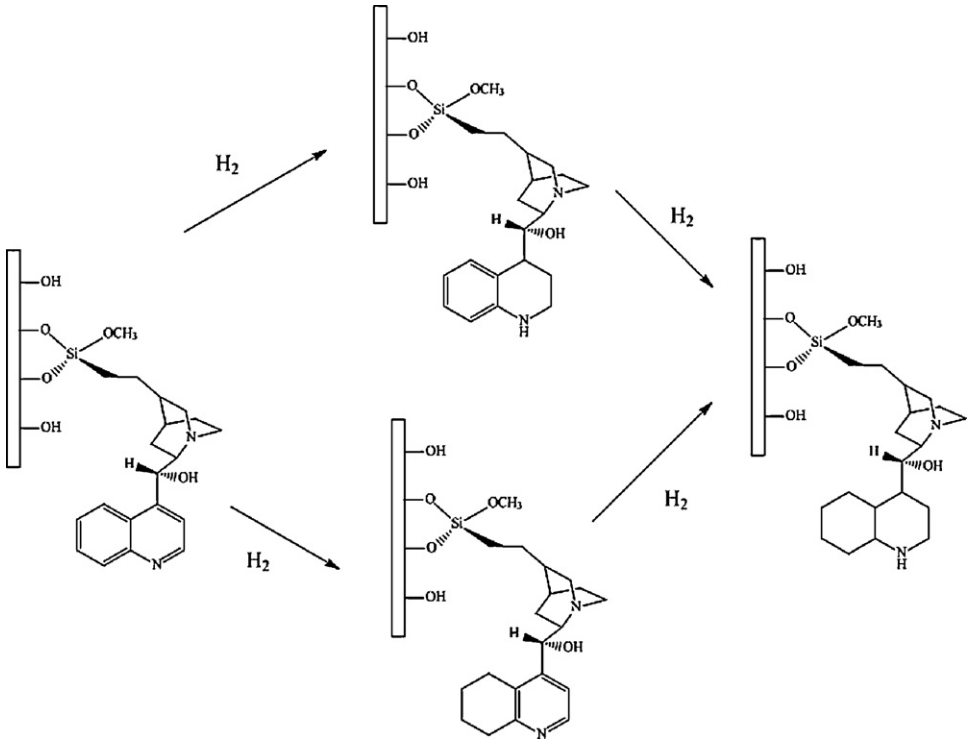

Scheme 4. Hydrogenation of the anchored inducer.

whereas the Pt/Si ratio decreases, attributed to a slight leaching of the metallic nanoparticles.

Fig. 11 shows the variations of conversion and ee as a function of the cycles studied. As the number of recycles increased, the activity decreased, falling to values of 88%, as shown in Table 6. Surface enrichment by undesired species on the support led, in the second cycle, to lower selectivity by the catalyst, interfering with the adsorption of the substrate on the modified active site. Consequently, hydrogenation at these sites produced a racemic mixture, decreasing the values of ee (see Table 6). In the third cycle, we detected the appearance of RR-diols, SS-diols, and *meso*-diols, as well as an ee that was attributed to the hydrogenation of the

Table 6
Catalytic data for cycles of the catalyst 1%Pt/SiCD(7.5). Reaction conditions: PPD concentration: 0.01 mol/L, catalyst mass: 0.050 g, P_{H_2} : 40 bar, stirring speed: 700 rpm.

Run	Conversion max (%)	ee[a] max (%)	ee[b] max (%)	rs max (%)	Concentration diols[a] (10^3 mol/L)
0	97	49	–	–	–
1	93	37	–	–	2.0
2	92	40	–	–	2.1
3	90	43	$47^{*,(30)}$	$54^{*,(90)}$	2.2
4	88	54	$45^{*,(15)}$	$55^{*,(30)}$	3.1

[a] ee referring to the C=O of the C1 of PPD.
[b] ee referring to the C=O of the C2 of PPD.
$^{*,(x)}$Maximum value of ee and rs considering x: time in which only the products 1-hydroxy-1-phenyl-propane-2-one and 2-hydroxy-1-phenyl-propane-1-one were observed.

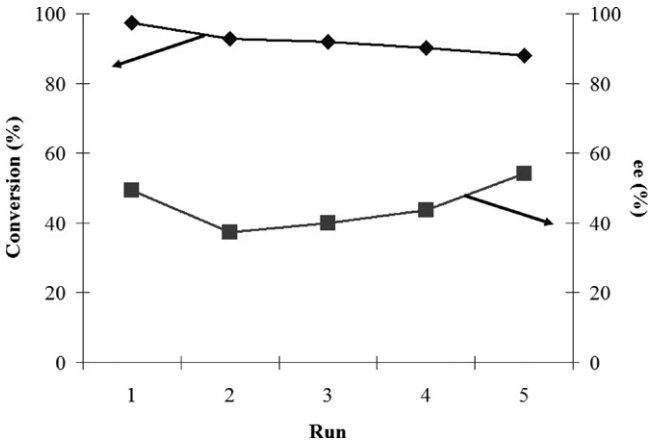

Fig. 11. Activity curves and ee in function of the number of reaction cycles for the catalyst 1%Pt/SiCD(7.5). Reaction conditions: PPD concentration: 0.01 mol/L, catalyst mass: 0.050 g, P_{H_2} : 40 bar, mixing speed: 700 rpm, solvent: cyclohexane.

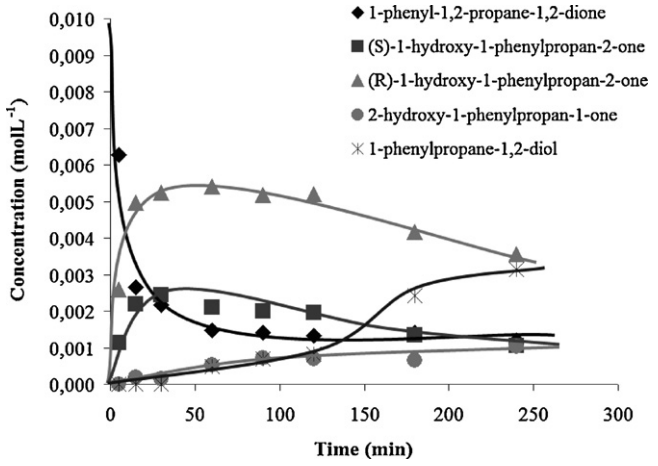

Fig. 12. Distribution of products in function of the time for cycle 5 of the catalyst 1%Pt/SiCD(7.5). Reaction conditions: PPD concentration: 0.01 mol/L, catalyst mass: 0.050 g, P_{H_2} : 40 bar, mixing speed: 700 rpm, solvent: cyclohexane.

hydroxy ketones, since the hydrogenation rate of 1S-FP is greater than that of 1R-FP, as reported by Toukoniitty et al. [7]. As the recycling was continued, these effects became more marked and the active sites became progressively less selective an in the last cycle (5th run) the decreases in the activity can be attributed to the leaching of the active phase as was detected by XPS (see Table 5). In cycles 4 and 5, we noted the appearance of the hydrogenation species of the C=O adjacent to the methyl group (see Scheme 2). We determined the ee[2] and rs in both cases (see Table 5), finding that the preferred products were those that had the absolute configuration R and the majority product in all the cases was 1R-FP, as shown in the distribution curve of reaction products for cycle 5 (Fig. 12). As the reaction time increased, the rs for 1R-FP and 1S-FP reached a maximum of ~50. After this, the appearance of diols caused the values of rs to decrease due to the hydrogenation rates of the corresponding hydroxy ketones that preferentially consumed 1S-FP, as can be seen in the increase of the ee[1] value.

4. Conclusions

It is possible to achieve structural modifications of CD to obtain a derivative that can be anchored on the surface of SiO_2 and to obtain supported metallic catalysts by the reduction of a metallic precursor under high pressure H_2. We observed textural and structural variations as the TMS-CD content increased on the supports. All the catalysts were active in the enantioselective hydrogenation of PPD and selective for 1R-FP. The most enantioselective was that which corresponded to a concentration of 0.75 mmol/L g. In consecutive batch cycles, this catalyst lost activity and enantioselectivity due to the interaction of the support with other species in the reaction system between catalytic cycles.

Acknowledgements

The authors thank FONDECYT Project 1061001 and Project AT-24091014.

References

[1] H.U. Blaser, B. Pugin, M. Studer, Chiral Catalyst Immobilization and Recycling, Wiley-VCH publishers, Toronto, 1998, pp. 6–15.
[2] A. Vargas, T. Bürgi, A. Baiker, J. Catal. 226 (2004) 691–692.
[3] J.P. Rasor, E. Voss, Appl. Catal. A: Gen. 221 (2001) 145–158.
[4] S.P. Griffiths, P. Johnston, P.B. Wells, Appl. Catal. A 191 (2000) 193–204.
[5] T. Burgi, A. Baiker, Acc. Chem. Res. 37 (2004) 909–917.
[6] E. Toukoniitty, B. Ševcíková, P. Mäki-Arvela, J. Wärnå, T. Salmi, D.Y. Murzin, J. Catal. 213 (2003) 7–16.
[7] E. Toukoniitty, P. Mäki-Arvela, A.K. Neyestanaki, R. Sjöholm, R. Leino, T. Salmi, D.Y. Murzin, React. Kinet. Catal. Lett. 75 (2002) 21–30.
[8] Y. Orito, S. Imai, S. Niwa, J. Chem. Soc. Jpn. 8 (1979) 1118–1121.
[9] C.E. Song, S.-G. Lee, Chem. Rev. 102 (2002) 3495–3524.
[10] J. Jamis, J.R. Anderson, R.S. Dickson, W.R. Jackson, J. Organomet. Chem. 627 (2001) 37.
[11] Q.-H. Fan, Y.-M. Li, A.S.C. Chan, Chem. Rev. 102 (2002) 3300–3385.
[12] R. Aldea, H. Alper, J. Organomet. Chem. 593–594 (2000) 454–457.
[13] S.V. Belyaev, E.F. Vainshtein, M.V. Klyuev, Kinet. Catal. 43 (2002) 245.
[14] D.E. Bergbreiter, Chiral Catalyst Immobilization and Recycling, Wiley-VCH publishers, Toronto, 1998, pp. 54–59.
[15] J.K.J. Stille, J. Macromol. Sci., Part A: Pure Appl. Chem. 24 (1984) 1689.
[16] I.F.J. Vakelecom, D. Tas, R.F. Parton, V. Vyver, P.A. Jacobs, Angew. Chem. Int. Ed. 35 (1996) 1346–1348.
[17] M. Lämmerhofer, W. Lindner, J. Chromatogr. A 741 (1996) 33–48.
[18] X. Ma, Y. Wang, W. Wang, J. Cao, Catal. Commun. 11 (2010) 401–407.
[19] A. Lindholm, P. Mäki-Arvela, E. Toukoniitty, T.A. Pakkanen, J.T. Hirvi, T. Salmi, D.Y. Murzin, R. Sjöholm, R. Leino, J. Chem. Perkin Trans. 12 (2002) 2605–2612.
[20] E. Toukoniitty, P. Mäki-Arvela, A.K. Neyestanaki, T. Salmi, R. Sjöholm, R. Leino, E. Laine, P.J. Kooyman, T. Ollonqvist, J. Väyrynen, Appl. Catal. A: Gen. 216 (2001) 73–83.
[21] C.-H. Chu, E. Jonsson, M. Auvinen, J.J. Pesek, J.E. Sandoval, Anal. Chem. 65 (1993) 808–816.
[22] J.E. Sandoval, J.J. Pesek, Anal. Chem. 61 (1989) 2067–2075.
[23] J.J. Cras, C.A. Rowe-Taitt, D.A. Nivens, F.S. Ligler, Biosens. Bioelectron. 14 (1999) 683–688.
[24] R.E. Fernandez, E. Bhattacharya, A. Chadha, Appl. Surf. Sci. 254 (2008) 4512–4519.
[25] E. Glickman, A. Inberg, N. Fishelson, Y. Shaham-Diamand, Microelectron. Eng. 84 (2007) 2466–2470.
[26] Y. Han, D. Mayer, A. Offenhäusser, S. Ingebrandt, Thin Solid Films 510 (2006) 175–180.
[27] N. Tokman, S. Akman, M. Ozcan, Talanta 59 (2003) 201–205.
[28] J.N. Volle, G. Chambon, A. Sayah, C. Reymond, N. Fasel, M.A.M. Gijs, Biosens. Bioelectron. 19 (2003) 457–464.
[29] K.M. Kacprzak, N.M. Maier, W. Lindner, Tetrahedron Lett. 47 (2006) 8721–8726.
[30] M.U. Azmat, Y. Guo, Y. Guo, Y. Wang, G. Lu, J. Mol. Catal. A: Chem. 336 (2011) 42–50.
[31] R.O. Pinho, E. Radovanovic, I.L. Torriani, I.V.P. Yoshida, Eur. Polym. J. 40 (2004) 615–622.
[32] E. Toukoniitty, P. Mäki-Arvela, J. Wärna, T. Salmi, Catal. Today 65 (2001) 411–417.
[33] E. Toukoniitty, B. Ševcíková, N. Kumar, P. Maki-Arvela, T. Salmi, J. Vayrynen, Stud. Surf. Sci. Catal. 135 (2001) 236.
[34] C. Burda, X. Chen, R. Narayanan, M.A. El-Sayed, Chem. Rev. 105 (2005) 1025–1102.
[35] H. Bönnemann, G. Braun, W. Brijoux, R. Brinkmann, A.S. Tilling, K. Seevogel, K. Siepen, J. Organomet. Chem. 520 (1996) 143–162.
[36] C.-W. Chen, D. Tano, M. Akashi, J. Colloid Interface Sci. 225 (2000) 349–358.
[37] H. Bönnemann, G.A. Braun, Angew. Chem. Int. Ed. 35 (1996) 1992–1995.
[38] V. Mévellec, C. Mattioda, J. Schulz, J.-P. Rolland, A. Roucoux, J. Catal. 225 (2004) 1–6.
[39] D. Ruiz, J.L.F. Fierro, P. Reyes, J. Braz. Chem. Soc. 21 (2010) 262–269.
[40] D. Ruiz, P. Reyes, J. Chil. Chem. Soc. 54 (2008) 1740–1746.
[41] C.D. Wagner, L.E. Davis, M.V. Zeller, J.A. Taylor, R.H. Raymond, L.H. Gale, Surf. Interface Anal. 3 (1981) 211–225.
[42] P. Reyes, C.H. Campos, J.L.G. Fierro, J. Chil. Chem. Soc. 52 (2007) 1126–1131.
[43] C.J. Zhou, R.F. Guan, S.Y. Feng, Eur. Polym. J. 40 (2004) 165–170.
[44] J. Blümel, J. Am. Chem. Soc. 117 (1995) 2112–2113.

[45] N. Fukaya, H. Haga, T. Tsuchimoto, S. Onozawa, T. Sakakura, H. Yasuda, J. Organomet. Chem. 695 (2010).
[46] P. Yu, J. He, L. Yang, M. Pu, X. Guo, J. Catal. 260 (2008) 81–85.
[47] M.A. Schiavon, S.U.A. Redondo, S.R.O. Pina, I.V.P. Yoshida, J. Non-Cryst. Solids 304 (2002) 92–100.
[48] M. Mirza-Aghayan, R. Boukherroub, M. Bolourtchian, J. Organomet. Chem. 690 (2005) 2372–2375.
[49] J.L. Margitfalvi, E. Tálas, Appl. Catal. A: Gen. 182 (1999) 65–74.
[50] P. Reyes, T. Marzialetti, J.L.G. Fierro, Catal. Today 107–108 (2005) 235–243.
[51] C. Urbina, G. Pecchi, C. Campos, P. Reyes, J. Chil. Chem. Soc. 54 (2010) 331–336.
[52] W.J. Gammon, O. Kraft, A.C. Reillya, B.C. Holloway, Carbon 41 (2003) 1917–1923.